

Symbol-Level Multiuser MISO Precoding for Multi-level Adaptive Modulation: A Multicast View

Maha Alodeh, *Student Member, IEEE*, Symeon Chatzinotas,
Senior Member, IEEE, Björn Ottersten, *Fellow Member, IEEE*

Maha Alodeh, Symeon Chatzinotas and Björn Ottersten are with Interdisciplinary Centre for Security Reliability and Trust (SnT) at the University of Luxembourg, Luxembourg. E-mails: { maha.alodeh@uni.lu, symeon.chatzinotas @uni.lu, and bjorn.ottersten@uni.lu }.

This work is supported by Fond National de la Recherche Luxembourg (FNR) projects, Smart Resource Allocation for Satellite Cognitive Radio (SRAT-SCR), Spectrum Management and Interference Mitigation in Cognitive Radio Satellite Networks (SeMiGod), and SATellite SEnsor NeTworks for spectrum monitoring (SATSENT). Part of this work is accepted in Globecom 2015, arXiv:1504.06750 [cs.IT]. This work is protected under the filed patent, System and Method for Symbol-level Precoding in Multiuser Broadcast Channels, EP No.: 15186548.2

Symbol-Level Multiuser MISO Precoding for Multi-level Adaptive Modulation: A Multicast View

Abstract

Symbol-level precoding is a new paradigm for multiuser downlink systems which aims at creating constructive interference among the transmitted data streams. This can be enabled by designing the precoded signal of the multiantenna transmitter on a symbol level, taking into account both channel state information and data symbols. Previous literature has studied this paradigm for MPSK modulations by addressing various performance metrics, such as power minimization and maximization of the minimum rate. In this paper, we extend this to generic multi-level modulations i.e. MQAM and APSK by establishing connection to PHY layer multicasting with phase constraints. Furthermore, we address adaptive modulation schemes which are crucial in enabling the throughput scaling of symbol-level precoded systems. In this direction, we design signal processing algorithms for minimizing the required power under per-user SINR or goodput constraints. Extensive numerical results show that the proposed algorithm provides considerable power and energy efficiency gains, while adapting the employed modulation scheme to match the requested data rate.

Index Terms

Symbol-level precoding, Constructive interference, Multiuser MISO Channel, MQAM, APSK.

I. INTRODUCTION

In a generic framework, precoding can be loosely defined as the design of the transmitted signal to efficiently deliver the desired information to multiple users exploiting the multiantenna space. Focusing on multiuser downlink systems, the precoding techniques can be classified as:

- 1) *Group-level precoding* in which multiple codewords are transmitted simultaneously but each codeword (i.e. a sequence of symbols) is addressed to a group of users. This case is also known as multigroup multicast precoding [1]- [4] and the precoder design is dependent on the channels in each user group.
- 2) *User-level precoding* in which multiple codewords are transmitted simultaneously but each codeword (i.e. a sequence of symbols) is addressed to a single user. This case is also known

as multi-antenna broadcast channel precoding [5]- [16] and the precoder design is dependent on the channels of the individual users.

- 3) *Symbol-level precoding* in which multiple symbols are transmitted simultaneously and each symbol is addressed to a single user [17]- [25]. This is also known as a constructive interference precoding and the precoder design is dependent on both the channels (CSI) and the symbols of the users.

It has been shown in various literature that symbol-level precoding shows considerable gains in comparison to the conventional group- or user-level precoding schemes [17]- [25]. The main reason is that in symbol-level precoding the vector of the aggregate multiuser interference can be manipulated, so that it contributes in a constructive manner from the perspective of each individual user. This approach cannot be exploited in conventional precoding schemes, since each codeword includes a sequence of symbols and the phase component of each symbol rotates the interference vector in a different direction. As a result, conventional schemes focus on controlling solely the power of the aggregate multiuser interference, neglecting the vector phase in the signal domain. However, it should be highlighted here that the anticipated symbol-level gains come at the expense of additional complexity at the system design level. More specifically, the precoded signal has to be recalculated on a symbol- instead of a codeword-basis. Therefore, faster precoder calculation and switching is requisite for symbol-level precoding, which can be translated to more complex algorithms at the transmitter side.

Before highlighting the contributions of this paper, the following paragraphs present a detailed overview of related work. The paradigm of constructive interference for multiuser MISO downlink was firstly proposed in [17], but it was strictly limited to PSK modulations. The main concept relies on the fact that the multiuser interference can be pre-designed at the transmitter, so that it steers the PSK symbol deeper into the correct detection region. Based on an MMSE objective, two techniques were proposed based on partial zero-forcing [17] and correlation rotation [18]. These techniques were based on decorrelating the user channels before designing the constructive interference. However, this step leads to suboptimal performance, as channel correlation can be beneficial while aiming for constructive interference. Based on this observation, an MRT-based solution was proposed in [21], which outperformed previous techniques.

All aforementioned techniques have a commonality, namely they were based on the conventional approach of applying a precoding matrix to the user symbol vector for designing the transmitted signal. Interestingly, authors in [21] [22] have shown that in symbol-level precoding

more efficient solutions can be found while designing the transmitted signal directly. Following this intuition, a novel multicast-based symbol-level precoding technique was initially proposed in [21] and later elaborated in [22] for MPSK modulations. In more detail, the transmitted signal can be designed directly by solving an equivalent PHY multicasting problem with additional phase constraints on the received user signal. Subsequently, the calculated complex coefficients can be utilized to modulate directly the output of each antenna instead of multiplying the desired user symbol vector with a precoding matrix. Based on this novel approach, authors in [23] have extended the multicast-based symbol-level precoding for imperfect CSI by proposing a robust precoding scheme.

Going one step further, the above techniques were generalized in [24] [25] taking into account that the desired MPSK symbol does not have to be constrained by a strict phase constraint for the received signal, as long as it remains in the correct detection region. The flexible phase constraints can obviously introduce a higher SER if not properly designed. In this direction, the work in [25] studies the optimal operating point in terms of flexible phase constraints that maximizes the system energy efficiency.

In the context of the above related work, the main contributions of this paper are:

- The extension of symbol-level precoding to multi-level modulations, such as MQAM and APSK.
- The definition of a system architecture for a symbol-level precoding transmitter.
- The extension of the connections between symbol-level precoding and phase-constrained PHY multicasting for generic multi-level modulations.
- The derivation of a symbol-level precoding algorithm for the power minimization with SINR or goodput constraints under an adaptive modulation scheme.

The remainder of this paper is organized as follows: the system model is described in section (II). A multicast characterization to symbol-level precoding is explained in section (III). In section (V), we propose a symbol-level precoding for multi-level modulation. Finally, the numerical results are displayed in section (VI).

Notation: We use boldface upper and lower case letters for matrices and column vectors, respectively. $(\cdot)^H$, $(\cdot)^*$ stand for Hermitian transpose and conjugate of (\cdot) . $\mathbb{E}(\cdot)$ and $\|\cdot\|$ denote the statistical expectation and the Euclidean norm, and $\mathbf{A} \succeq \mathbf{0}$ is used to indicate the positive semidefinite matrix. $\angle(\cdot)$, $|\cdot|$ are the angle and magnitude of (\cdot) respectively. $Re(\cdot)$, $Im(\cdot)$ are the real and the imaginary parts of (\cdot) .

II. SYSTEM AND SIGNAL MODELS

Let us consider a single-cell multiple-antenna downlink scenario, where a single BS¹ is equipped with M transmit antennas that serves K user terminals, each one of them is equipped with a single receiving antenna². As depicted in Fig. 1, the transmission scheme is based on K frames (one per user) which include a common preamble for the pilot symbols and signaling information, followed by N useful symbols for each user (data payload). It should be noted that the preamble is not precoded, while the useful symbols are precoded on a symbol-level.

Similar to conventional multiuser precoding schemes, the pilots are exploited by each user in order to estimate its channel through standard CSI estimation methods and feed it back to the BS, so that it can be used in the design of the precoded signal. In this context, we assume a quasi static block fading channel $\mathbf{h}_j \in \mathbb{C}^{1 \times M}$ between the BS antennas and the j^{th} user³. This is assumed to be known at the BS based on the CSI feedback and fixed for each frame, i.e. N symbols.

Regarding the useful symbols, the BS can serve each user with a different modulation to support different levels of user rates. This is enabled through an adaptive modulation scheme, which can be concisely described by the Table 1. In more detail, the modulation for each user is selected from the set $\mathcal{M} = \{1, \dots, M\}$ based on the user's requested rate and the SINR min and max thresholds of Table 1. The supported SINR range is $\gamma \in [\gamma_0, \gamma_{\max}]$ and thus, SINRs lower than γ_0 lead to unavailability (i.e. zero goodput), while SNRs larger than γ_{\max} do not provide a further goodput increase.

It should be noted that although the precoding changes on a symbol-basis, the modulation types are allocated to users on a frame-basis. This is necessary because the user expects to receive the same modulation type for all useful symbols in a frame in order to properly adjust the detection regions. The users are notified about their corresponding modulations through the signaling preamble of the frame⁴.

¹The described system can be straightforwardly extended for a multicell system where the signal design takes place in a centralized manner, e.g. Coordinated MultiPoint (CoMP), Cloud Radio Access Network (RAN) etc.

²The MIMO case is briefly discussed in section III-C

³The proposed algorithms can be applied to Very High Speed Digital Subscriber Line (VDSL), where the channel remains constant for a long period [12]

⁴Changing the modulation on a symbol-basis is unfeasible, as the user would have to be notified about the used modulation on a symbol-basis and this would lead to unacceptable overhead.

Modulation Index m	1	2	\dots	M
min SINR	γ_0	γ_1	\dots	γ_{M-1}
max SINR	γ_1	γ_2	\dots	γ_{\max}
Supported rate (bits/symbol)	R_1	R_2	\dots	R_M

TABLE I
ABSTRACTION OF AN ADAPTIVE MODULATION SCHEME.

For a single symbol period $n = 1 \dots N$, the received signal at j^{th} user can be written as

$$y_j[n] = \mathbf{h}_j \mathbf{x}[n] + z_j[n]. \quad (1)$$

$\mathbf{x}[n] \in \mathbb{C}^{M \times 1}$ is the transmitted symbol sampled signal vector at the n th symbol period from the multiple antennas transmitter and z_j denotes the noise at j th receiver, which is assumed as an i.i.d complex Gaussian distributed variable $\mathcal{CN}(0, \sigma_z^2)$. A compact formulation of the received signal at all users' receivers can be written as

$$\mathbf{y}[n] = \mathbf{H} \mathbf{x}[n] + \mathbf{z}[n]. \quad (2)$$

Assuming linear precoding, let $\mathbf{x}[n]$ be written as $\mathbf{x}[n] = \sum_{j=1}^K \mathbf{w}_j[n] d_j[n]$, where \mathbf{w}_j is the $\mathbb{C}^{M \times 1}$ precoding vector for user j . The received signal at j^{th} user y_j in n^{th} symbol period is given by

$$y_j[n] = \mathbf{h}_j \mathbf{w}_j[n] d_j[n] + \sum_{k \neq j} \mathbf{h}_j \mathbf{w}_k[n] d_k[n] + z_j[n]. \quad (3)$$

A more detailed compact system formulation is obtained by stacking the received signals and the noise components for the set of K selected users as

$$\mathbf{y}[n] = \mathbf{H} \mathbf{W}[n] \mathbf{d}[n] + \mathbf{z}[n] \quad (4)$$

with $\mathbf{H} = [\mathbf{h}_1, \dots, \mathbf{h}_K]^T \in \mathbb{C}^{K \times M}$, $\mathbf{W} = [\mathbf{w}_1, \dots, \mathbf{w}_K] \in \mathbb{C}^{M \times K}$ as the compact channel and precoding matrices. Notice that the transmitted symbol vector $\mathbf{d} \in \mathbb{C}^{K \times 1}$ includes the uncorrelated data symbols d_k for all users with $\mathbb{E}_n[|d_k|^2] = 1$. From now on, we drop the symbol period index for the sake of notation.

The power constraint can be expressed for each symbol vector transmission as $\|\mathbf{x}\|^2 = \text{tr}(\mathbf{W} \mathbf{d} \mathbf{d}^H \mathbf{W}^H) = \|\sum_{j=1}^K \mathbf{w}_j d_j\|^2$.

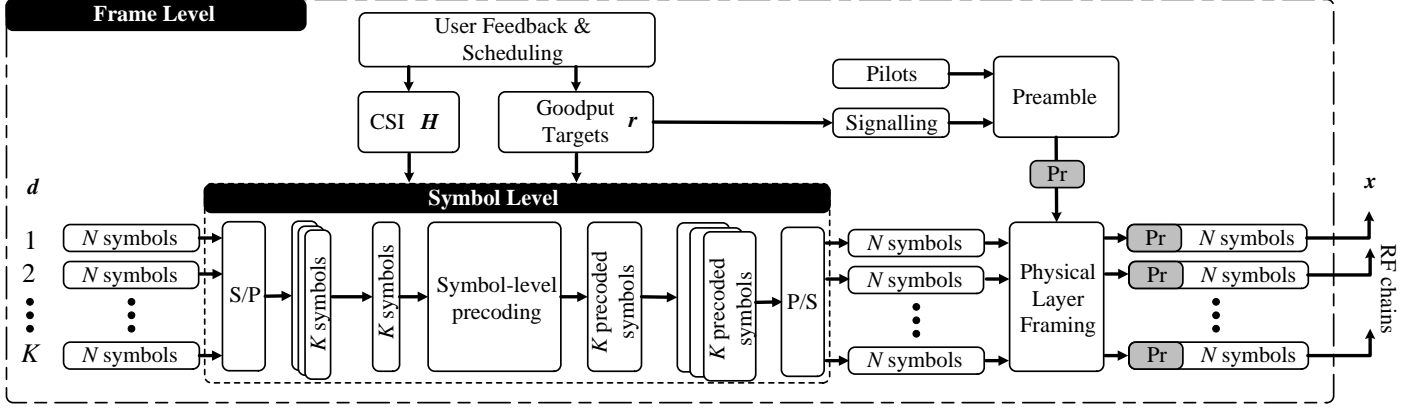


Fig. 1. Transmitter block diagram for symbol-level precoding. The block operations are classified into frame-level and symbol-level.

III. MULTICAST APPROACH TO SYMBOL-LEVEL PRECODING

A. PHY-layer Multicasting Preliminaries

The PHY-layer multicasting aims at sending a single message to multiple users simultaneously through multiple transmit antennas [27]- [30]. In this context, the power min problem for PHY-layer multicasting can be written as:

$$\begin{aligned} \mathbf{x}(\mathbf{H}, \boldsymbol{\zeta}) &= \arg \min_{\mathbf{x}} \|\mathbf{x}\|^2 \\ s.t. \quad &\|\mathbf{h}_j \mathbf{x}\|^2 = \zeta_j \sigma_z^2, \forall j \in K \end{aligned} \quad (5)$$

where ζ_j is the SINR target for the j^{th} user that should be granted by the BS, and $\boldsymbol{\zeta} = [\zeta_1, \dots, \zeta_K]$ is the vector that contains all the SINR targets. This problem has been efficiently solved using semidefinite relaxation [33] in [27].

B. Symbol-level Precoding Through Multicasting

Let us define a generic constellation represented by the symbol set \mathcal{D} , where $d_j \in \mathcal{D}$ represent symbols (see Fig. (2)). Each symbol can have two equivalent representations:

- 1) Magnitude $|d_j|^2$ and phase $\angle(d_j)$
- 2) In-phase $Re\{d_j\}$ and quadrature $Im\{d_j\}$ components.

Let us also denote the received signal at the antenna of the j th user (ignoring the receiver noise) as $\mathbf{s}_j = \mathbf{h}_j \sum_{k=1}^K \mathbf{w}_k d_k$. In this context, a generic formulation for power minimization in a single

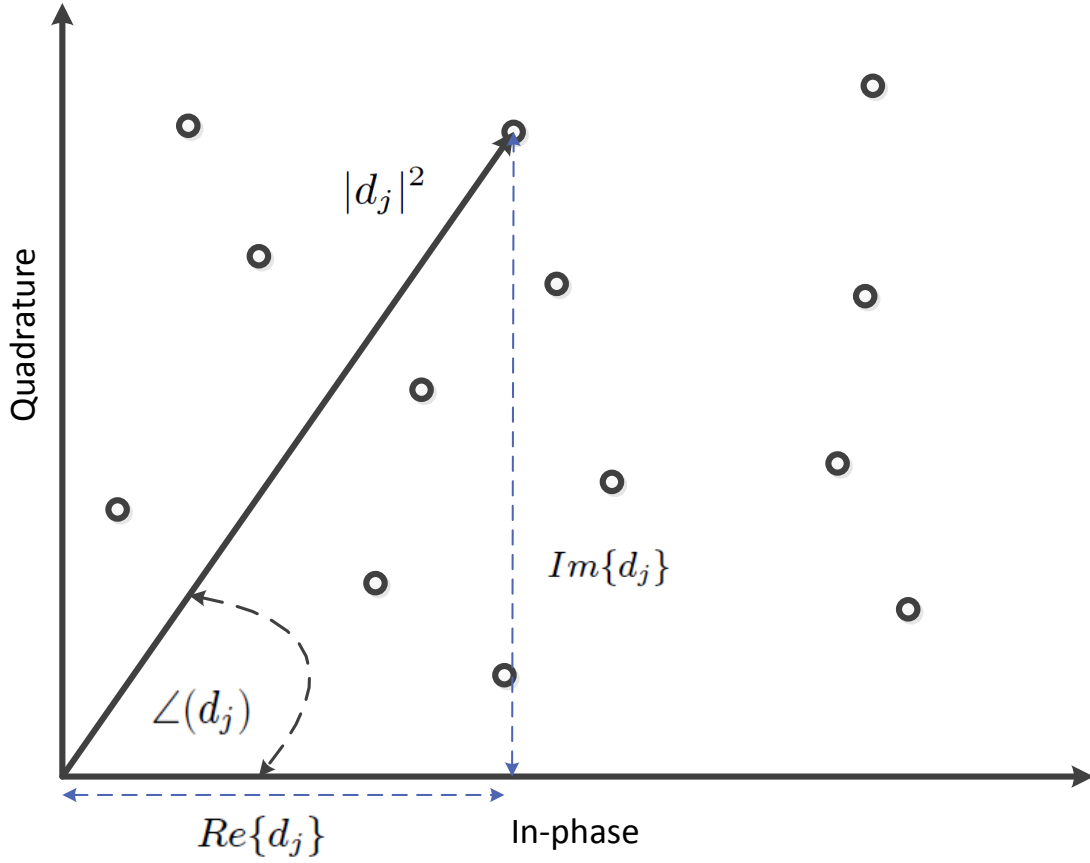


Fig. 2. The first quadrant of a generic modulation constellation.

symbol period under symbol-level precoding and SINR constraints⁵ can be written using the I-Q

⁵The complete algorithm including goodput constraints is elaborated in section V-B.

representation:

$$\begin{aligned}
\mathbf{w}_k(\mathbf{d}, \mathbf{H}, \zeta) &= \arg \min \left\| \sum_{k=1}^K \mathbf{w}_k d_k \right\|^2 \\
s.t. \quad \mathcal{C}_1 : \mathcal{I}\{\mathbf{h}_j \sum_{k=1}^K \mathbf{w}_k d_k\} &= \kappa_j \sqrt{\zeta_j} \sigma_z \text{Re}\{d_j\}, \forall j \in K \\
\mathcal{C}_2 : \mathcal{Q}\{\mathbf{h}_j \sum_{k=1}^K \mathbf{w}_k d_k\} &= \kappa_j \sqrt{\zeta_j} \sigma_z \text{Im}\{d_j\}, \forall j \in K
\end{aligned} \tag{6}$$

Using the magnitude-phase representation, an equivalent way of formulating the problem can be expressed as:

$$\begin{aligned}
\mathbf{w}_k(\mathbf{d}, \mathbf{H}, \zeta) &= \arg \min \left\| \sum_{k=1}^K \mathbf{w}_k d_k \right\|^2 \\
s.t. \quad \mathcal{C}_1 : \left\| \mathbf{h}_j \sum_{k=1}^K \mathbf{w}_k d_k \right\|^2 &= \kappa_j^2 \zeta_j \sigma_z^2, \forall j \in K \\
\mathcal{C}_2 : \angle(\mathbf{h}_j \sum_{k=1}^K \mathbf{w}_k d_k) &= \angle(d_j), \forall j \in K
\end{aligned} \tag{7}$$

The set of constraints $\mathcal{C}_1, \mathcal{C}_2$ guarantees that each user receives its corresponding data symbol d_j with a correct amplitude and phase⁶. The desired amplitude for each user depends on two factors: a long and a short-term one. The long-term factor refers to the target SINR ζ which determines the SER and remains constant across all the symbol vectors of a frame. The short-term factor $\kappa_j = |d_j| / \sqrt{\mathbb{E}_{\mathcal{D}}[|d_j|^2]}$ changes on a symbol-basis and adjusts the long-term SINR based on the amplitude of the desired symbol. Assuming that the entire symbol set \mathcal{D} has unit average power i.e. $\mathbb{E}_{\mathcal{D}}[|d_j|^2] = 1$, κ_j denotes the scaling factor needed for the magnitude of the desired symbol with respect to the average power of the entire symbol set.

Theorem 1. *In symbol-level precoding, the power minimization problem under SINR constraints (7) is equivalent to a PHY-layer multicasting problem with an effective channel $\hat{\mathbf{H}}$ and phase constraints (10).*

Proof: Before starting the proof, it should be noted that the variable amplitude of each target symbol has been already incorporated in the SINR constraints of \mathcal{C}_1 . In other words, the

⁶ \mathcal{C}_1 and \mathcal{C}_2 depend on the type of modulation and the constellation point as elaborated in section IV.

multi-level amplitudes for each user have been expressed as weighting factors for the frame-level SNRs ζ . Building on this, the proof is based on two steps: a) defining an effective channel, where each symbol phase is absorbed in the user's channel vector, b) observing that the transmitted signal vector \mathbf{x} can be designed directly and not as a linear product of the precoding matrix with the symbol vector i.e. $\mathbf{W}\mathbf{d}$.

By denoting the contribution of each user's precoded symbol to the transmit signal as $\mathbf{x}_k = \mathbf{w}_k d_k$, and assuming a unit-norm symbol d with a reference phase, let us define the effective channel $\hat{\mathbf{H}} = \mathbf{A}\mathbf{H}$, where \mathbf{A} is a diagonal $K \times K$ matrix expressed as:

$$[\mathbf{A}]_{j,j} = \exp(\angle(d - d_j)i) \quad (8)$$

Using the above notations, an equivalent optimization problem can be formulated below:

$$\begin{aligned} \mathbf{x}_k(\hat{\mathbf{H}}, \zeta) &= \arg \min \left\| \sum_{k=1}^K \mathbf{x}_k \right\|^2 \\ s.t. \quad \mathcal{C}_1 : & \left\| \hat{\mathbf{h}}_j \sum_{k=1}^K \mathbf{x}_k \right\|^2 = \kappa_j^2 \zeta_j \sigma_z^2, \forall j \in K \\ \mathcal{C}_2 : & \angle(\hat{\mathbf{h}}_j \sum_{k=1}^K \mathbf{x}_k) = \angle(d), \forall j \in K. \end{aligned} \quad (9)$$

It should be noted that the original user symbols do not appear in the optimization problem anymore, as they have been incorporated in the weighted SNR constraints and the effective channel. Based on this observation, we can go one step further and design directly the transmit signal \mathbf{x} , by dropping its dependency on the individual user's symbols. Replacing $\mathbf{x} = \sum_{j=1}^K \mathbf{x}_j$ yields:

$$\begin{aligned} \mathbf{x}(\hat{\mathbf{H}}, \zeta) &= \arg \min \|\mathbf{x}\|^2 \\ s.t. \quad \mathcal{C}_1 : & \left\| \hat{\mathbf{h}}_j \mathbf{x} \right\|^2 = \kappa_j^2 \zeta_j \sigma_z^2, \forall j \in K \\ \mathcal{C}_2 : & \angle(\hat{\mathbf{h}}_j \mathbf{x}) = \angle(d), \forall j \in K. \end{aligned} \quad (10)$$

which is equivalent to a PHY-layer multicasting problem (5) for the effective channel $\hat{\mathbf{H}}$ with additional phase constraints on the received user signals \mathcal{C}_2 . ■

Corollary 1. *An equivalent formulation of the optimization problem (7) can be expressed by rewriting the magnitude and phase constraints in the form of in-phase and quadrature constraints:*

$$\begin{aligned} \mathbf{x}(\hat{\mathbf{H}}, \zeta) &= \arg \min \|\mathbf{x}\|^2 \\ \mathcal{C}_1 : \quad \mathcal{I}_j &= \kappa_j \sqrt{\zeta_j} \sigma_z \operatorname{Re}\{d\}, \forall j \in K \\ \mathcal{C}_2 : \quad \mathcal{Q}_j &= \kappa_j \sqrt{\zeta_j} \sigma_z \operatorname{Im}\{d\}, \forall j \in K, \end{aligned} \quad (11)$$

where \mathcal{I}_j , \mathcal{Q}_j are in-phase and out-of-phase components for the detected signal at j^{th} terminal and can be reformulated as:

$$\begin{aligned} \mathcal{I}_j &= \frac{\hat{\mathbf{h}}_j \mathbf{x} + (\hat{\mathbf{h}}_j \mathbf{x})^*}{2} \\ \mathcal{Q}_j &= \frac{\hat{\mathbf{h}}_j \mathbf{x} - (\hat{\mathbf{h}}_j \mathbf{x})^*}{2i}. \end{aligned}$$

Remark 1. *The PHY-layer multicasting problem in (5) is based on constraints in the power domain (amplitude only), while the symbol-level precoding problems in (10) and (12) are based on constraints in the signal domain (both amplitude and phase). This lower-level optimization is enabled by the fact that the all components (both symbols and channel) that affect the user received signal are taken into account in symbol-level precoding.*

C. Multiple Antennas at the Receivers

Let us assume a multiuser downlink system where each user is equipped with an arbitrary number of antennas. As it can be seen, the signal model in (4) can be straightforwardly adopted for the multiantenna receivers, considering that each element of \mathbf{y} is the received signal at a single antenna instead of a single user. Assuming that the SINR constraints ζ apply for each user antenna the analysis in the previous section also follows straightforwardly for optimizing the transmit signal vector \mathbf{x} . More importantly, since each antenna can receive the desired symbol without multi-stream or multi-user interference, there is no need for jointly processing the streams received by the multiple antennas of each user.

IV. SYMBOL-LEVEL PRECODING WITH MULTI-LEVEL MODULATION

For practical constellations, we can rewrite the constraints \mathcal{C}_1 and \mathcal{C}_2 to exploit the specific detection regions which depend on the type of modulation and the constellation point. In the

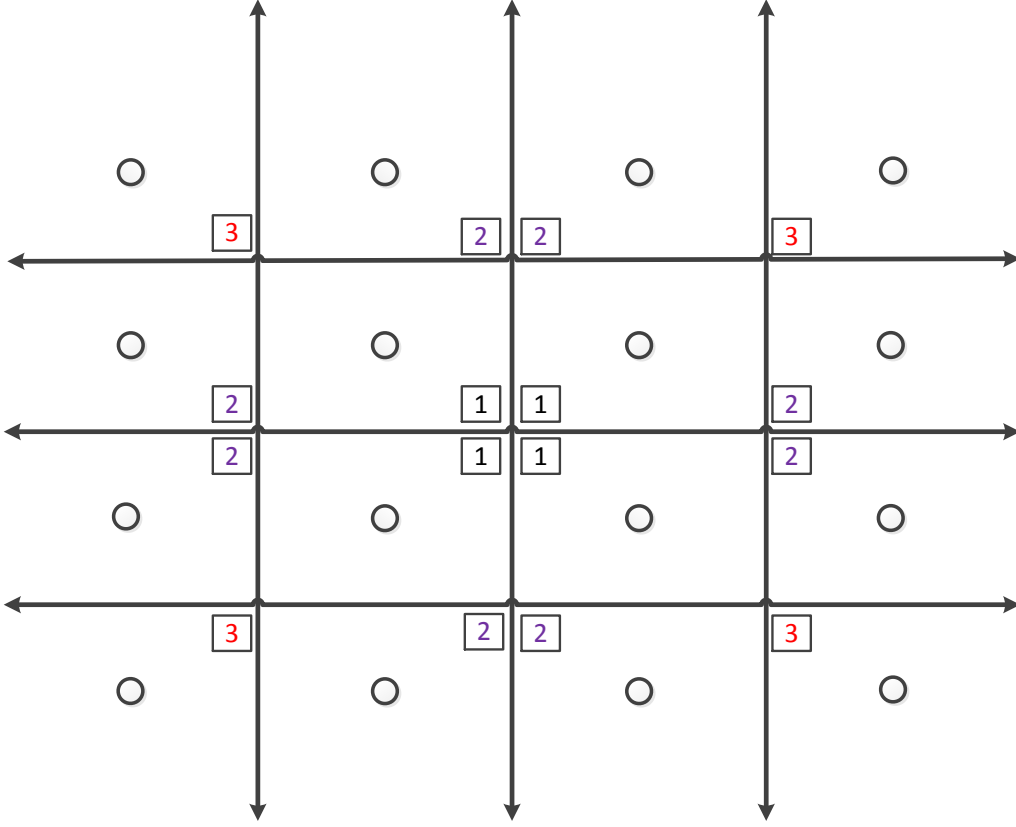


Fig. 3. Classification of the constellation points for a 16-QAM modulation into inner(1), outer(2) and outermost(3).

following paragraphs, we specify the constraints for a number of typical modulation types, but the same rationale can be straightforwardly applied to other modulation types.

A. MQAM

For MQAM (see Fig. 3), detailed expressions for \mathcal{C}_1 , \mathcal{C}_2 can be written as

- For the inner-constellation symbols, the constraints \mathcal{C}_1 , \mathcal{C}_2 should guarantee that the received signals achieve the exact constellation point. For 16-QAM as depicted in Fig. (3), the symbols marked by 1 should be received with the exact symbols. The constraints can be written as

$$\mathcal{C}_1 : \mathcal{I}_j = \sqrt{\zeta_j} \kappa_j \sigma_z \text{Re}\{d_j\}$$

$$\mathcal{C}_2 : \mathcal{Q}_j = \sqrt{\zeta_j} \kappa_j \sigma_z \text{Im}\{d_j\}$$

- Outer constellation symbols, the constraints $\mathcal{C}_1, \mathcal{C}_2$ should guarantee the received signals lie in the correct detection. For 16-QAM as depicted in Fig. (3), the symbols marked by 2 should be received with the exact symbols. The constraints can be written as

$$\mathcal{C}_1 : \mathcal{I}_j \begin{smallmatrix} \geq \\ \leq \end{smallmatrix} \sqrt{\zeta_j \kappa_j \sigma_z} \text{Re}\{d_j\}$$

$$\mathcal{C}_2 : \mathcal{Q}_j = \sqrt{\zeta_j \kappa_j \sigma_z} \text{Im}\{d_j\}$$

$$\mathcal{C}_1 : \mathcal{I}_j = \sqrt{\zeta_j \kappa_j \sigma_z} \text{Re}\{d_j\}$$

$$\mathcal{C}_2 : \mathcal{Q}_j \begin{smallmatrix} \geq \\ \leq \end{smallmatrix} \sqrt{\zeta_j \kappa_j \sigma_z} \text{Im}\{d_j\},$$

- Outermost constellation symbols, the constraints $\mathcal{C}_1, \mathcal{C}_2$ should guarantee the received signals lie in the correct detection. For 16-QAM as depicted in Fig. (3), the symbols marked by 3 should be received with the exact symbols. The constraints can be written as

$$\mathcal{C}_1 : \mathcal{I}_j \begin{smallmatrix} \geq \\ \leq \end{smallmatrix} \sqrt{\zeta_j \kappa_j \sigma_z} \text{Re}\{d_j\}$$

$$\mathcal{C}_2 : \mathcal{Q}_j \begin{smallmatrix} \geq \\ \leq \end{smallmatrix} \sqrt{\zeta_j \kappa_j \sigma_z} \text{Im}\{d_j\}.$$

The sign $\begin{smallmatrix} \geq \\ \leq \end{smallmatrix}$ indicates that the symbols should locate in the correct detection region, for the symbols in the first quadrant $\begin{smallmatrix} \geq \\ \leq \end{smallmatrix}$ means \geq .

Following the same rationale, $\mathcal{C}_1, \mathcal{C}_2$ can be defined for any MQAM constellation.

B. APSK

For APSK, detailed expression for $\mathcal{C}_1, \mathcal{C}_2$ can be written as

- For inner constellation point, $\mathcal{C}_1, \mathcal{C}_2$ should assure that the received signals should be received at the exact constellation point. The constraints can be expressed as

$$\mathcal{C}_1 : \mathcal{I}_j = \sqrt{\zeta_j \kappa_j \sigma} \text{Re}\{d_j\}$$

$$\mathcal{C}_2 : \mathcal{Q}_j = \sqrt{\zeta_j \kappa_j \sigma} \text{Im}\{d_j\}$$

- Outermost constellation symbols, the constraints $\mathcal{C}_1, \mathcal{C}_2$ and \mathcal{C}_3 should guarantee the received signals lie in the correct detection. For 16 APSK as depicted in Fig. (4), the symbols marked by 2.

$$\mathcal{C}_1 : \sqrt{\mathcal{I}_j^2 + \mathcal{Q}_j^2} \geq \sqrt{\zeta_j \kappa_j \sigma_z}$$

$$\mathcal{C}_2 : \tan\left(\frac{\mathcal{Q}_j}{\mathcal{I}_j}\right) = \tan(\angle d_j)$$

$$\mathcal{C}_3 : \text{sign}(\mathcal{Q}_j) = \text{sign}(\text{Im}\{d_j\}) \quad (12)$$

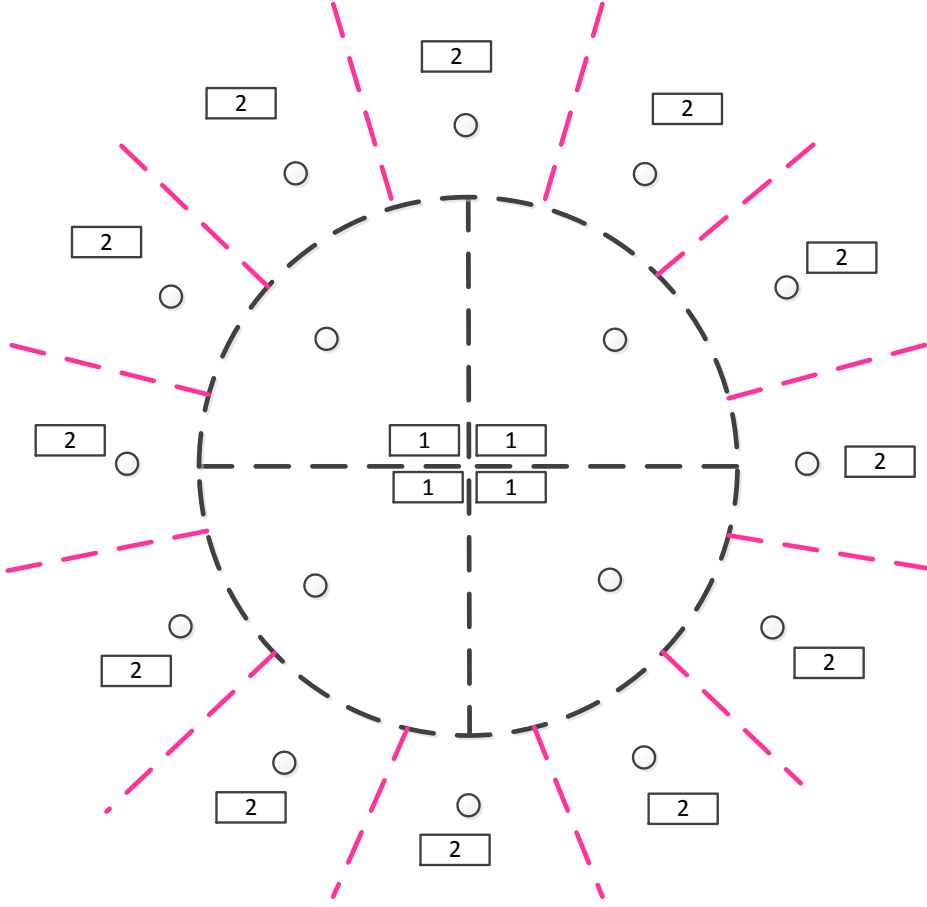


Fig. 4. Classification of the constellation points for a 16-APSK modulation into inner(1) and outer(2).

Following the same rationale, \mathcal{C}_1 , \mathcal{C}_2 can be defined for any APSK constellation by including one or more levels of inner symbols (i.e. equality constraints) as needed.

1) *Special case* : Any MPSK modulation can be implemented by a single layer APSK constellation. The constraints can be expressed [22] by setting $\kappa_j = 1$ as:

$$\begin{aligned}\mathcal{I}_j &= \sqrt{\zeta_j} \sigma_z \text{Re}\{d_j\}, \quad \forall j \in K, \\ \mathcal{Q}_j &= \sqrt{\zeta_j} \sigma_z \text{Im}\{d_j\}, \quad \forall j \in K.\end{aligned}\tag{13}$$

Remark 2. The outermost points of multi-level modulations (e.g. denoted by 3 in Fig.3 and 2 in Fig.4) have more flexible detection regions, since the symbol can be received correctly even it moves deeper into the detection region. This concept has been thoroughly investigated in [21] [22] for MPSK, where it was shown that this flexibility can lead to performance gains. In the previous sections, the same has been straightforwardly extended for multi-level modulations by

using inequalities for the in-phase and quadrature constraints of the outermost symbols (see sec.IV-A,IV-B). However, it should be noted that as we move into higher order constellations the effect of this flexibility is expected to diminish due to the large number of equality constraints. In these cases, the performance gain arises mainly from the multicast view rather than the flexible detection regions.

V. SYMBOL LEVEL POWER MINIMIZATION

The problem of power minimization has been addressed in numerous papers in the literature [5]- [6]. In the vast majority of previous works, the constraints were expressed in terms of SINR, since there is a straightforward connection between the SINR ζ and throughput rate R when Gaussian coding is assumed:

$$R_j = \log_2(1 + \zeta_j). \quad (14)$$

However, when symbol-level precoding is employed in combination with adaptive multi-level modulation, this simple analytical connection ceases to apply. In this case, the effective throughput rate or goodput⁷ \bar{R} depends on:

- the assigned modulation m , which sets the upper bound on the supported rate R in number of bits per symbol according to Table I
- the achieved SINR ζ_j , which determines the operating point on the SER curve

and it is expressed by :

$$\bar{R}_j = f(m_j, SER(\zeta_j)) = R_j(m_j)(1 - SER(\zeta_j, m_j)). \quad (15)$$

Now let us denote the consumed power for each of the N symbol vectors in a frame as $P[n], n = 1 \dots N$. The objective is to minimize the total power consumed while transmitting the whole frame, i.e. $\sum_{i=1}^N P[n]$. Assuming symbol-level precoding with adaptive multi-level modulation, the frame power minimization problem with goodput constraints can be expressed as:

$$\min_{\mathbf{x}} \sum_{i=1}^N P[n] = \sum_{i=1}^N \min_{\mathbf{x}[n]} P[n] \quad (16)$$

⁷These two terms are used interchangeably across this paper.

given that the power constraint is applied on a symbol vector basis. Dropping the symbol index n , for each symbol vector the transmitted precoded signal that minimizes the power $P = \|\mathbf{x}\|^2$ has to be calculated as:

$$\mathbf{x} = \arg \min_{\mathbf{x}} \|\mathbf{x}\|^2 \quad s.t. \quad \mathcal{C}_1, \mathcal{C}_2, \forall j \in K. \quad (17)$$

where $\mathcal{C}_1, \mathcal{C}_2$ are the set of constraints defined in previous section.

Remark 3. *The above problem is always feasible, as the power can scale freely to ensure that the SINR constraints can be satisfied for all effective channels resulting from different symbol vectors in a frame.*

In the following sections, we first address the power minimization problem with SINR constraints $\mathcal{C}_1, \mathcal{C}_2$ and then we build on it to develop a solution with goodput constraints $\bar{R}_j \geq r_j$, where \bar{R}_j, r_j are the effective rates and target rates (throughput) respectively.

A. Power Minimization with SINR Constraints (CIPM)

The power minimization with SINR constraints can be expressed as:

$$\begin{aligned} \mathbf{x} = \min_{\mathbf{x}} \quad & \|\mathbf{x}\|^2 \\ s.t. \quad & \mathcal{C}_1, \mathcal{C}_2 \quad \forall j \in K \end{aligned} \quad (18)$$

For any practical modulation scheme, the above problem can be solved by constructing appropriate $\mathcal{C}_1, \mathcal{C}_2$ constraints as explained in sec. IV. Subsequently, an equivalent channel can be constructed and \mathbf{x} can be straightforwardly calculated using Theorem III-B. The Lagrange function of (12), (18) can be expressed as:

$$\begin{aligned} \mathcal{L}(\mathbf{x}) = \mathbf{x}^H \mathbf{x} &+ \sum_j \lambda_j (\mathcal{I}_j(\mathbf{x}) - \sqrt{\zeta_j} \kappa_j \sigma_z \text{Re}\{d_j\}) \\ &+ \sum_j \mu_j (\mathcal{Q}_j(\mathbf{x}) - \sqrt{\zeta_j} \kappa_j \sigma_z \text{Im}\{d_j\}). \end{aligned} \quad (19)$$

The derivative of $\mathcal{L}(\mathbf{x})$ with respect to \mathbf{x}^* , λ_j , and μ_j can be expressed:

$$\frac{\partial \mathcal{L}(\mathbf{x})}{\partial \mathbf{x}^*} = \mathbf{x} + \sum_j \lambda_j \frac{d\mathcal{I}_j(\mathbf{x})}{d\mathbf{x}^*} + \sum_j \mu_j \frac{d\mathcal{Q}_j(\mathbf{x})}{d\mathbf{x}^*}, \quad (20)$$

$$\frac{\partial \mathcal{L}(\mathbf{x})}{\partial \lambda_j} = \mathcal{I}_j(\mathbf{x}) - \sqrt{\zeta_j} \kappa_j \sigma_z \text{Re}\{d_j\}, \quad (21)$$

$$\frac{\partial \mathcal{L}(\mathbf{x})}{\partial \mu_j} = \mathcal{Q}_j(\mathbf{x}) - \sqrt{\zeta_j} \kappa_j \sigma_z \text{Im}\{d_j\}. \quad (22)$$

By setting $\frac{\partial \mathcal{L}(\mathbf{x})}{\partial \mathbf{x}^*} = 0$, $\frac{\partial \mathcal{L}(\mathbf{x})}{\partial \lambda_j} = 0$, and $\frac{\partial \mathcal{L}(\mathbf{x})}{\partial \mu_j} = 0$, we can formulate the following set of equations:

$$\mathbf{x} = \sum_j -\lambda_j \frac{d\mathcal{I}_j(\mathbf{x})}{d\mathbf{x}^*} + \sum_j -\mu_j \frac{d\mathcal{Q}_j(\mathbf{x})}{d\mathbf{x}^*}, \quad (23)$$

$$\mathcal{I}_j(\mathbf{x}) = \sqrt{\zeta_j} \kappa_j \sigma_z \text{Re}\{d_j\}, \quad (24)$$

$$\mathcal{Q}_j(\mathbf{x}) = \sqrt{\zeta_j} \kappa_j \sigma_z \text{Im}\{d_j\}. \quad (25)$$

Using (23)-(25), the solution of (18) can be found by solving the set of equations as follows:

$$\mathcal{I}_j \left(\sum_j -\lambda_j \frac{d\mathcal{I}_j(\mathbf{x})}{d\mathbf{x}^*} + \sum_j -\mu_j \frac{d\mathcal{Q}_j(\mathbf{x})}{d\mathbf{x}^*} \right) = \sqrt{\zeta_j} \kappa_j \sigma_z \text{Re}\{d_j\}, \forall j \in K \quad (26)$$

$$\mathcal{Q}_j \left(\sum_j -\lambda_j \frac{d\mathcal{I}_j(\mathbf{x})}{d\mathbf{x}^*} + \sum_j -\mu_j \frac{d\mathcal{Q}_j(\mathbf{x})}{d\mathbf{x}^*} \right) = \sqrt{\zeta_j} \kappa_j \sigma_z \text{Im}\{d_j\}, \forall j \in K. \quad (27)$$

B. Power Minimization with Goodput Constraints

The power minimization with goodput constraints can be expressed as:

$$\begin{aligned} \mathbf{x} = \min_{\mathbf{x}} \quad & \|\mathbf{x}\|^2 \\ \text{s.t.} \quad & \bar{R}_j \geq r_j \forall j \in K. \end{aligned} \quad (28)$$

The rationale of the proposed algorithm can be summarized in the following steps:

- 1) The first step in solving this problem is allocating a modulation type m for each user. Based on the adaptive modulation rules of table I, we select the lowest modulation that can achieve the target goodput of each user.

$$R_{l-1} \leq r_j \leq R_l \text{ iff } m_j = l \quad (29)$$

- 2) In the second step, the goodput constraints r can be converted into SINR constraints ζ , given that the modulation types m have been already fixed. This can be performed by exploiting the analytical connection between the SER and the SINR. In more detail, the required SER for a specific goodput constraint r is given by:

$$\text{SER}(\zeta, m) = 1 - r/R(m), \quad (30)$$

and the required SINR for MQAM is expressed as a function of SER as follows [34]:

$$\zeta \leq \frac{2^R - 1}{3R} \left(Q^{-1} \left(\frac{\text{SER}}{4} \right) \right)^2. \quad (31)$$

Acronym	Technique	equation
CIPM	Constructive Interference- Power Minimization	(18)
Multicast	Optimal Multicast	(5), [27]
OB	Optimal user level beamforming	(35), [5]

TABLE II

SUMMARY OF THE PROPOSED, STATE-OF-THE-ART ALGORITHMS AND THE THEORETICAL LOWER BOUND, THEIR RELATED ACRONYMS, AND THEIR RELATED EQUATIONS AND ALGORITHMS

For MPSK, the required SINR for a specific goodput and SER constraints as [34]:

$$\zeta = \frac{1}{2 \sin^2(\frac{\pi}{2R})} \left(Q^{-1} \left(\frac{SER}{2} \right) \right)^2 \quad (32)$$

For APSK, various approximations can be used [35] or as an alternative, numerically calculated SER vs. SINR curves can be utilized in practical systems.

- 3) As a result, the power min under goodput constraints has been transformed into a power min under SINR constraint and this can be efficiently solved by the algorithm in section V-A.

C. Multiple Antennas at the Receivers

Assuming that goodput constraints applies for each antenna instead of each user, the above algorithm can be straightforwardly extended for multi-antenna receivers. However, when a goodput constraint apply for each user, there can be multiple combinations of per-antenna goodput constraints to be considered. In this case, the constraint in (28) is written as:

$$\sum_{a=1}^A \bar{R}_{j,a} \geq r_j, \forall j \quad (33)$$

assuming that the j th user has A antennas, and $\bar{R}_{j,a}$ is the effective rate of the j th user's antenna a .

VI. NUMERICAL RESULTS

Before discussing the numerical results, let us denote 1) the symbol-level power consumption by $P = \|\sum_{k=1}^K \mathbf{w}_k d_k\|^2 = \|\mathbf{x}\|^2$ and 2) the frame-level power consumption (average over over a large number of symbols) by $\bar{P} = \mathcal{E}_d[P]$. Let us also define the system energy efficiency as:

$$\eta = \frac{\sum_{j=1}^K \bar{R}_j(SER_j, m_j)}{\bar{P}} \quad (34)$$

which is going to be used as an additional performance metric that combines the system goodput with the required power. For the sake of comparison with an achievable user-level precoding method, we use the power minimization objective for user-level linear beamforming which is defined as:

$$\begin{aligned} \mathbf{w}_K = \arg \min & \quad \sum_{j=1}^K \|\mathbf{w}_j\|^2 \\ \text{s.t.} & \quad \frac{\|\mathbf{h}_j \mathbf{w}_j\|^2}{\sum_{k \neq j, k=1}^K \|\mathbf{h}_j \mathbf{w}_k\|^2 + \sigma_z^2} \geq \zeta_j, \forall j \in K. \end{aligned} \quad (35)$$

This problem has been efficiently solved in the literature [5]. It should be noted here that the above user-level precoders are calculated only once per frame and are subsequently applied unaltered to all input symbol vectors. In this direction, the target is to minimize the average power per frame under average SINR constraints. On the contrary, the proposed CIPM algorithm minimizes the instantaneous transmit power per input symbol vector and guarantees that the target SINR is achieved for each input symbol vector. As a result, a higher energy efficiency can be achieved while ensuring the SER across the whole frame. As a theoretical bound (lower-bound for transmission power and upper-bound for energy efficiency), we utilize the PHY-layer multicasting [27] as in (5).

For 8-QAM, the constraints \mathcal{C}_1 , \mathcal{C}_2 for each symbol can be written in detail as

$$\begin{aligned} \mathcal{C}_1 &= \begin{cases} \mathcal{I}_j = \sigma_z \sqrt{\frac{\zeta_j}{3}} \text{Re}\{d_j\}, d_j = \frac{\pm 1 \pm i}{\sqrt{2}} \\ \mathcal{I}_j \geq \sigma_z \sqrt{\frac{\zeta_j}{3}} \text{Re}\{d_j\}, d_j = \frac{3+i}{\sqrt{2}}, \frac{3-i}{\sqrt{2}} \\ \mathcal{I}_j \leq \sigma_z \sqrt{\frac{\zeta_j}{3}} \text{Re}\{d_j\}, d_j = \frac{-3+i}{\sqrt{2}}, \frac{-3-i}{\sqrt{2}} \end{cases} \\ \mathcal{C}_2 &= \begin{cases} \mathcal{Q}_j \geq \sigma_z \sqrt{\frac{\zeta_j}{3}} \text{Im}\{d_j\}, d_j = \frac{\pm 1+i}{\sqrt{2}}, \frac{\pm 3+i}{\sqrt{2}}, \\ \mathcal{Q}_j \leq \sigma_z \sqrt{\frac{\zeta_j}{3}} \text{Im}\{d_j\}, d_j = \frac{\pm 1-i}{\sqrt{2}}, \frac{\pm 3-i}{\sqrt{2}} \end{cases} \end{aligned}$$

For the 16-QAM modulation, the constraints \mathcal{C}_1 , \mathcal{C}_2 can be expressed as

$$\mathcal{C}_1 = \begin{cases} \mathcal{I}_j = \sigma_z \sqrt{\frac{\zeta_j}{5}} \text{Re}\{d_j\}, d_j = \frac{\pm 1 \pm i}{\sqrt{2}}, \frac{\pm 1 \pm 3i}{\sqrt{2}} \\ \mathcal{I}_j \geq \sigma_z \sqrt{\frac{\zeta_j}{5}} \text{Re}\{d_j\}, d_j = \frac{3+i}{\sqrt{2}}, \frac{3-i}{\sqrt{2}}, \frac{3+3i}{\sqrt{2}}, \frac{3-3i}{\sqrt{2}} \\ \mathcal{I}_j \leq 2\sigma_z \sqrt{\frac{\zeta_j}{5}} \text{Re}\{d_j\}, d_j = \frac{-3+i}{\sqrt{2}}, \frac{-3-i}{\sqrt{2}}, \frac{-3+3i}{\sqrt{2}}, \frac{-3-3i}{\sqrt{2}} \end{cases}$$

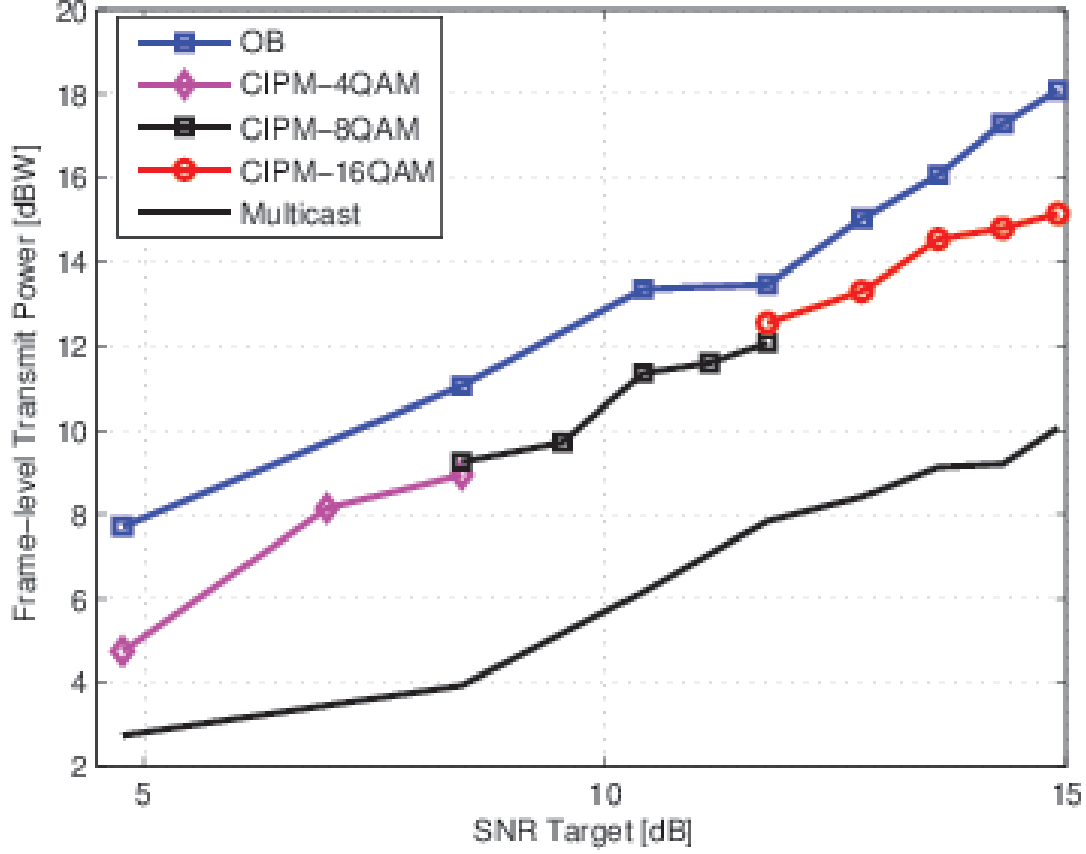


Fig. 5. Frame-level Transmit Power in dBW vs target SINR in dB $\sigma_h^2 = 10$ dB, $\sigma_z^2 = 0$ dB.

$$\mathcal{C}_2 = \begin{cases} Q_j = \sigma_z \sqrt{\frac{\zeta_j}{5}} \text{Im}\{d_j\}, d_j = \frac{\pm 1 + \pm i}{\sqrt{2}}, \frac{\pm 3 + \pm i}{\sqrt{2}}, \\ Q_j \geq \sigma_z \sqrt{\frac{\zeta_j}{5}} \text{Im}\{d_j\}, d_j = \frac{\pm 1 + 3i}{\sqrt{2}}, \frac{\pm 3 + 3i}{\sqrt{2}} \\ Q_j \leq \sigma_z \sqrt{\frac{\zeta_j}{5}} \text{Im}\{d_j\}, d_j = \frac{\pm 1 - 3i}{\sqrt{2}}, \frac{\pm 3 - 3i}{\sqrt{2}} \end{cases}$$

The presented results in Fig. (5)-(7) have been acquired by averaging over 50 frames of $N = 100$ symbols each. A quasi-static block fading channel was assumed where each block corresponds to a frame and the fading coefficients were generated as $\mathbf{H} \sim \mathcal{CN}(0, \sigma_h^2 \mathbf{I})$.

Fig. (5) compares the performance between optimal user-level beamforming, symbol-level precoding, and PHY-layer multicasting from an average transmit power perspective. In all cases, the power minimization under SINR constraints is considered. The PHY-multicasting presents a theoretical lower-bound for CIPM since it does not have the phase constraints required to grant

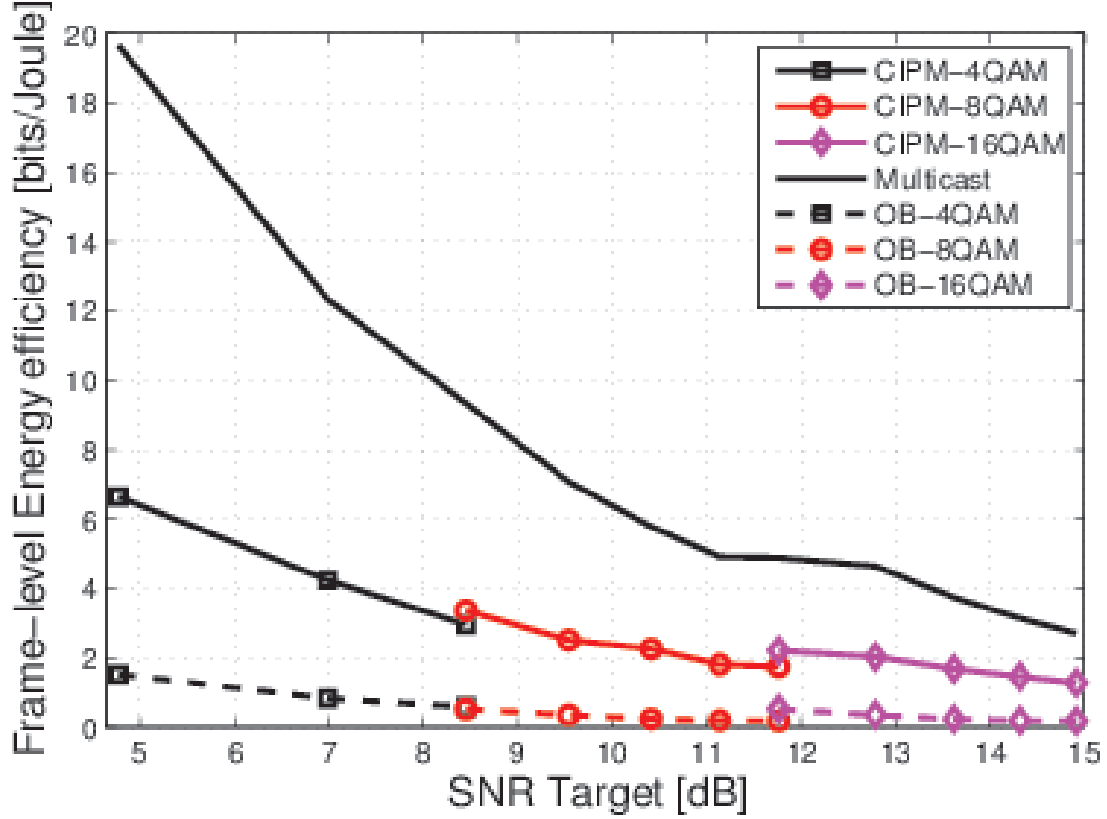


Fig. 6. Frame-level energy efficiency vs target SINR $\sigma_h^2 = 10$ dB, $\sigma_z^2 = 0$ dB

the constructive reception of the multiuser interference, while it can be noted that symbol-level precoding (CIPM) outperforms the optimal user-level precoding at every SINR target. This can be explained by the way we tackle the interference. In OB, the interference is mitigated to grant the SINR target constraints. In CIPM, the interference is exploited at each symbol to reduce the required power to achieve the SINR targets. Furthermore, it can be noted that the throughput of CIPM can be scaled with the SINR target by employing adaptive multi-level modulation (4/8/16-QAM).

Fig. (6) compares the performance between optimal user-level beamforming, symbol-level precoding, and PHY-layer multicasting from an energy efficiency perspective. It can be noted that CIPM outperforms OB at all target SINR values. This can be explained by the decreased required power to achieve the SINR target since the energy efficiency takes into the account both goodput and power consumption.

Fig. (7) compares OB and CIPM in terms of frame-level transmit power scaling versus system

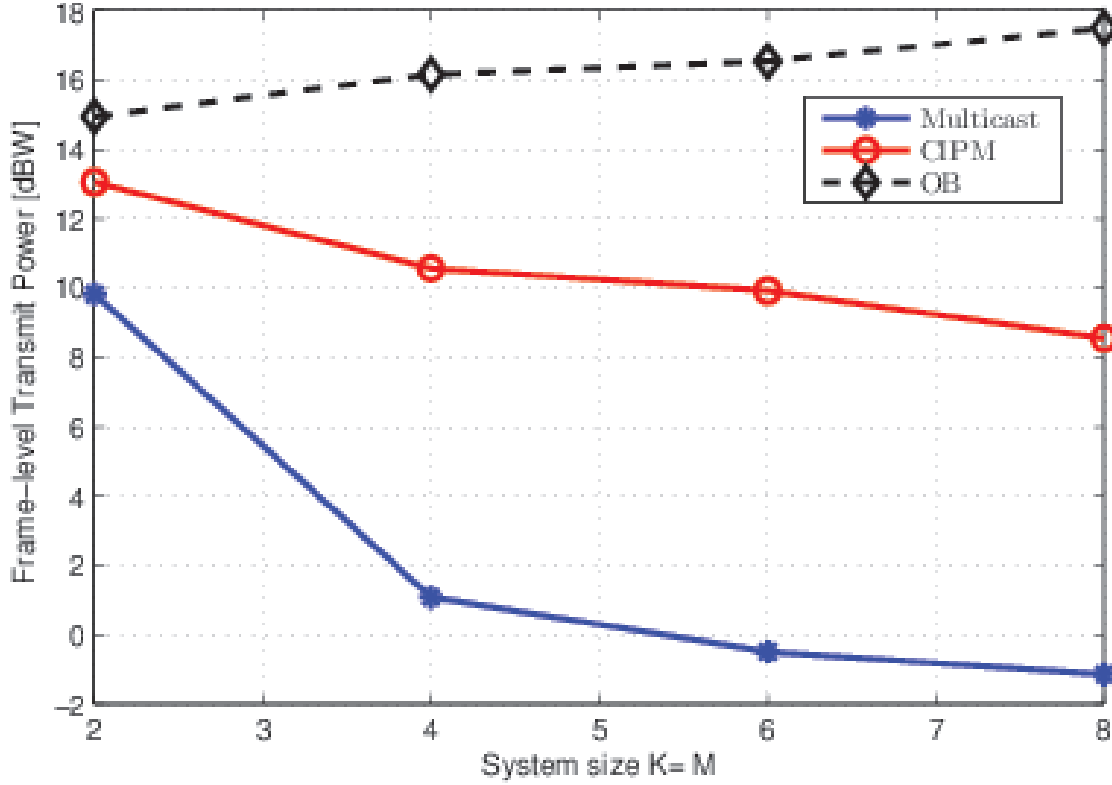


Fig. 7. Frame-level transmit power vs the number of the system size, $K = M$, 16QAM, $\sigma_h^2 = 10$ dB, $\sigma_z^2 = 0$ dB.

size. It should be reminded that the energy efficiency metric takes into the account the detection errors at the receiver. It can be noted that the average transmit power for CIPM decreases with the system size, while for OB it increases. This can be explained intuitively by the fact that the power leaving each transmit antenna constructively contributes to achieve the SINR targets for each user. On the contrary, OB has to send a higher number of interfering symbol streams as the system size increases and this leads to poor energy efficiency.

Fig. (8) depicts the power variation during the frame for CIPM and OB. We study the transmit power at all possible symbol combinations, which is equal to 16 combinations for 2×2 system size and QPSK for both users. It should be noted that channels between the BS and users' terminal are fixed during the frame, the users' channels have the following value:

$$\mathbf{H} = \begin{bmatrix} 0.1787 + 1.9179i & 0.9201 + 1.0048i \\ -2.1209 - 1.5455i & 1.5138 + 0.2250i \end{bmatrix}$$

The long term average OB equals to $\sum_{i=1}^2 \|\mathbf{w}_i\|^2$, average OB equals to $\mathbb{E}_{d_j} \|\sum_{i=1}^2 \mathbf{w}_i d_i\|^2$ and

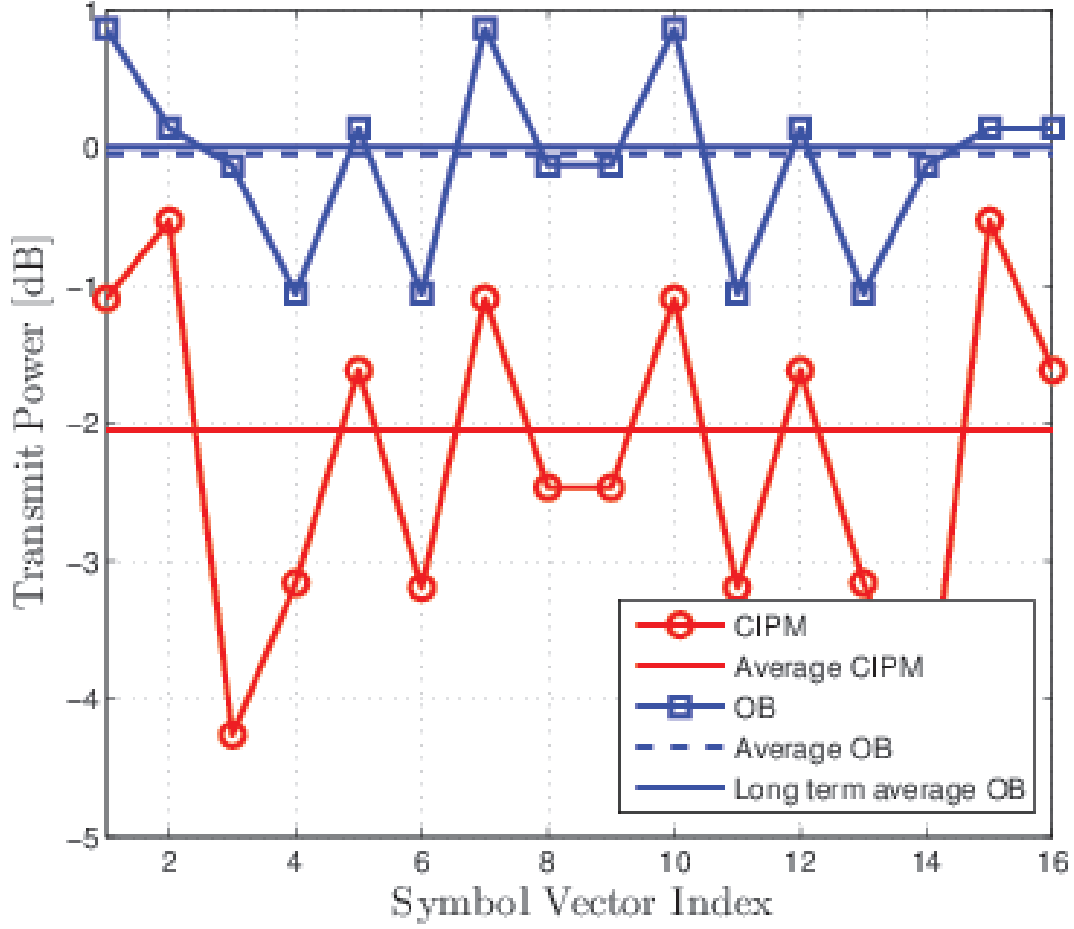


Fig. 8. The power variance during the frame, QPSK modulation. $M = 2$, $K = 2$, $\sigma_h^2 = 10$ dB, $\sigma_z^2 = 0$ dB.

OB $\|\sum_{i=1}^2 \mathbf{w}_i d_i\|^2$. It can be noted that the average transmit power per frame for OB is 2.2 dB higher than CIPM. The power changes within the frame. It can be noted that the maximum power difference between CIPM and OB equals to 4.1 dB at symbol combination no. 3 and no. 14 and the minimum power difference equals to 0.4 dB at symbol combination no. 2 and no. 15.

In Fig. (9)-(10), we depict the transmit power and the energy efficiency regions for the following 2×2 channel:

$$\mathbf{H} = \begin{bmatrix} 1.3171 + 5.6483i & -1.8960 + 0.6877i \\ -0.6569 + 3.7018i & -2.5047 - 2.8110i \end{bmatrix}$$

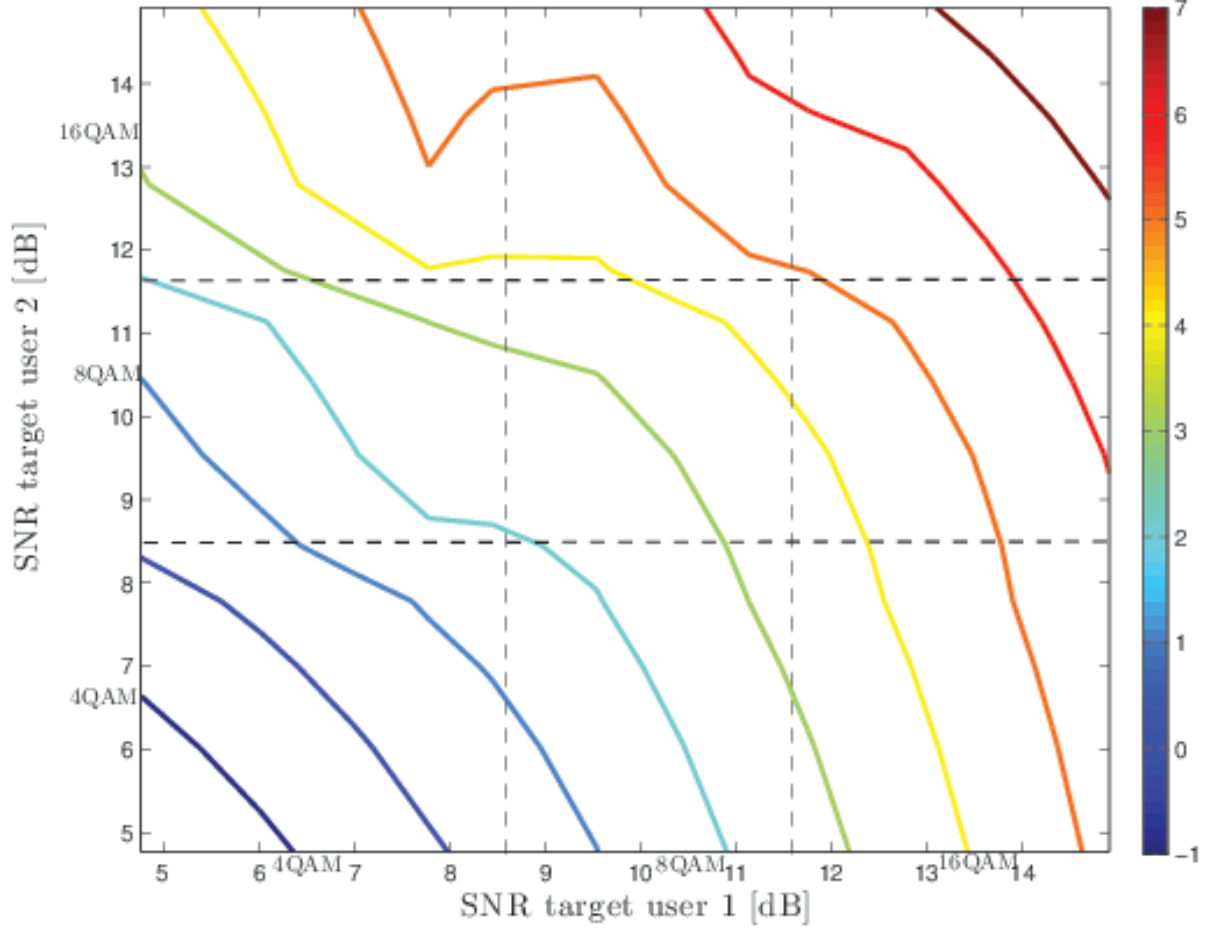


Fig. 9. Transmit power regions vs users' target SINR and their corresponding modulation. $M = 2$, $K = 2$, $\sigma_h^2 = 10$ dB, and $\sigma_z^2 = 0$ dB.

In Fig. (9), we illustrate the transmit power with respect to SINR target constraints (and their mapping to the corresponding modulation). At each SINR constraint set, we find the average power for all possible symbol combinations. It should be noted that symbol-level precoding can satisfy different data rate requirements by assigning different modulations to different users. Moreover, it can be noted that the transmit power increases with increasing the modulation order since this demands higher target SINR.

In Fig. (10), we plot the energy efficiency with respect to SINR target constraints (and their mapping to the corresponding modulation). At each SINR constraints set, we find the energy efficiency for all possible symbol combinations. For each symbol combination and SINR

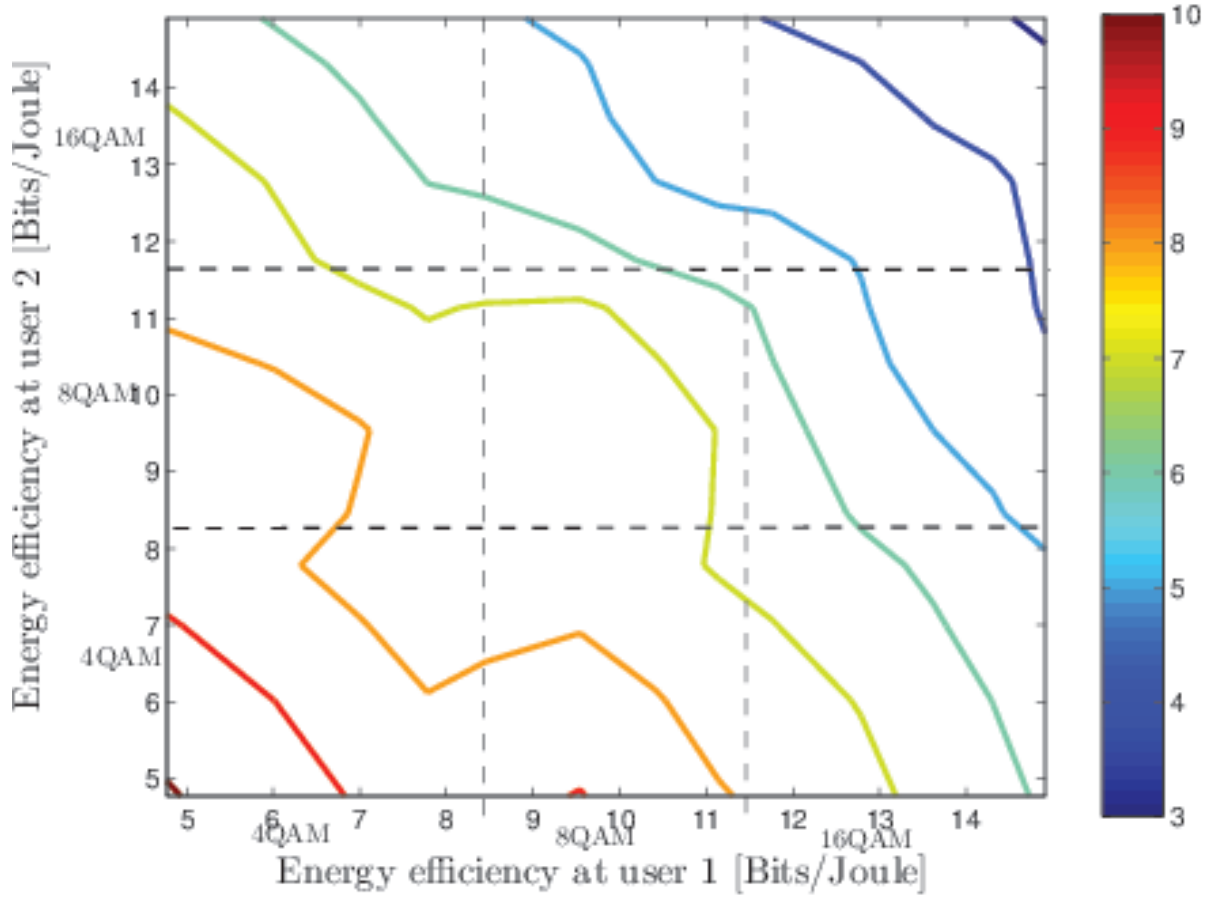


Fig. 10. Energy efficiency regions η vs users' target SINR and their corresponding modulation. $M = 2$, $K = 2$, $\sigma_h^2 = 10$ dB, and $\sigma_z^2 = 0$ dB.

constraint, we vary the noise to capture the impact of SER on the energy efficiency performance. It can be noted that the energy efficiency decreases with increasing the modulation order since this demands higher target SINR.

SER is depicted in Fig. (11) for 4QAM and 16QAM modulations. If we assume that the target rates for user 1 and user 2 are 3.6 bps/Hz , and 1.998 bps/Hz respectively, the modulation types that suit the rate requirements imposed by each user are 16 QAM and 4 QAM respectively. Based on (30), the corresponding SER for both users are 10^{-1} , 10^{-3} respectively. Using the SER values, we can find the related SINR target constraints from the curves in Fig. (11), which are almost 13 dB and 10 db respectively.

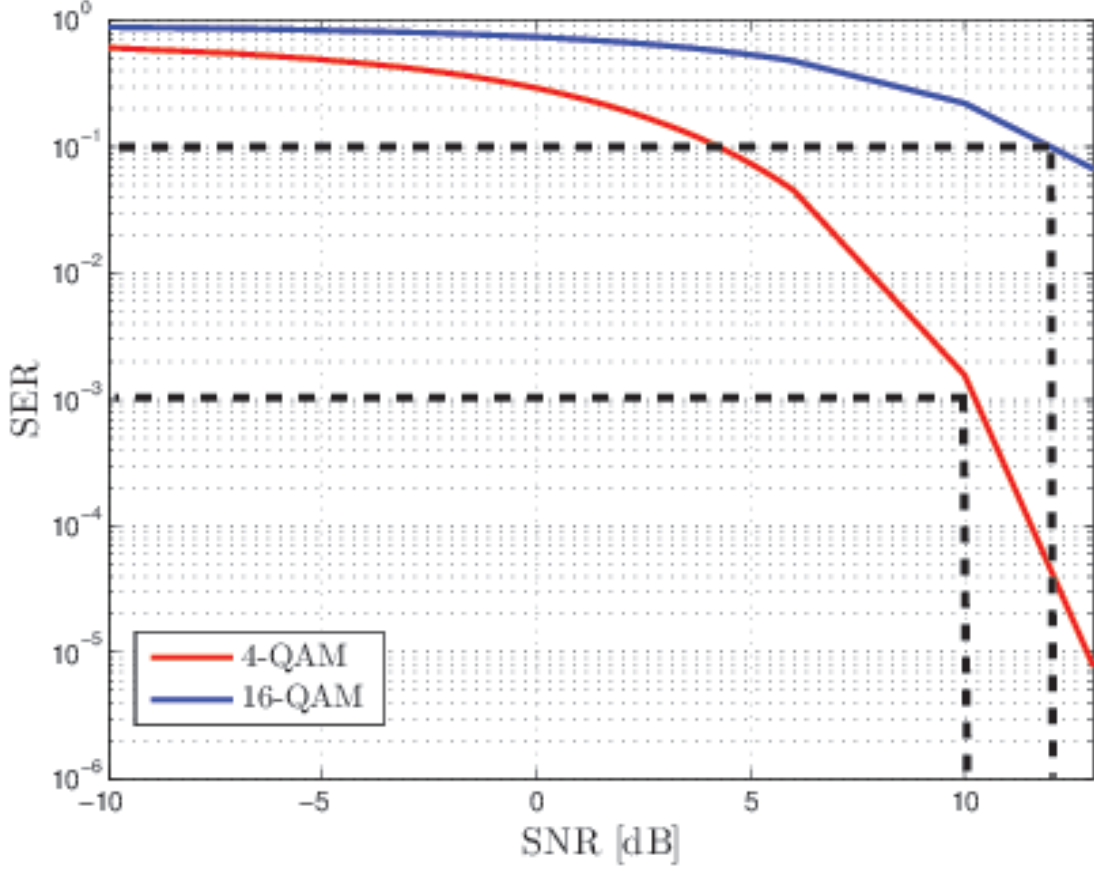


Fig. 11. SER curves vs SNR for 4-QAM and 16-QAM. The dashed lines present the selected SNR targets to achieve the SER value of 10^{-3} , 10^{-1} for 4-QAM and 16-QAM respectively.

Technique/ $(M \times K)$	(2×2)	(3×3)	(4×4)	(5×5)
OB	0.2090	0.2512	0.3421	0.3674
CIPM	$0.312 \times \kappa_2$	$0.360 \times \kappa_3$	$0.407 \times \kappa_4$	$0.370 \times \kappa_5$

TABLE III

COMPARISON OF THE DIFFERENT TECHNIQUE FROM SIMULATION RUN TIME PERSPECTIVE. $\sigma_h^2 = 20dB$, $\zeta = 4.712dB$, QPSK, $\kappa_2 = 2^{2 \times 2}$, $\kappa_3 = 2^{3 \times 2}$, $\kappa_4 = 2^{4 \times 2}$, $\kappa_5 = 2^{5 \times 2}$.

A. Complexity

The source of complexity in the symbol-level precoding is the number of possible precoding calculations within a frame. This depends on the number of users, the modulation order of each user and the frame length N . The number of the possible calculations \mathcal{N} can be mathematically

expressed:

$$\mathcal{N} = \min\{2^{\sum_{j=1}^K m_j}, N\}. \quad (36)$$

For small systems (i.e. lower modulation order and small K), the precoding vector can be evaluated beforehand on a frame-level for all possible symbol vector combinations and employed when required in the form of a lookup table. For large system (i.e. high order modulation order, high number of users), the number of the possible calculations in some cases is less than the frame length, so it is not necessary to find the precoding for all the possible combinations.

At each symbol combination, a convex optimization is solved. The complexity of such operation is evaluated using the simulation run-time metric as a metric. The complexity of the proposed algorithm is studied in Table (III) in terms of simulation run-time. We compared the run-time of optimal beamforming (OB) and different symbol-level precoding. From the table, it can be deduced that the run time for OB is the lower than CIPM as expected. Moreover, the run-time for symbol-level precoding techniques depends on the combinations of the modulation order (possible data symbols) and the number of users, which is explained by the factor κ_x in the table. However, for a single solution of the optimization problem, it can be seen that CIPM is less complex than OB as system size increases. Despite the high complexity of the proposed technique, it can be argued that with the emerging of cloud RAN, this computational complexity can be transferred to the cloud RAN level [36].

VII. CONCLUSIONS

Symbol-level precoding that jointly utilizes the CSI and data symbols to exploit the multiuser interference has been proposed for multi-level modulation. In these cases, the precoding design exploits the overlap in users' subspace instead of mitigating it. In this work, we proposed precoding techniques that extend the concept of symbol-level precoding to adaptive multi-level constellation. This is a crucial step in order to enable the throughput scaling in symbol-level precoded systems. More specifically, we have generalized the relation between the symbol-level precoding and PHY-layer multicasting with phase constraints for any generic modulation. To assess the gains, we compared the symbol-level precoding to conventional user-level precoding techniques. For 2×2 scenario, a 2.2 dB transmit power reduction has been achieved. More importantly, this performance gain increases with the system size. Therefore, it can be conjectured that the symbol-level precoding retains some performance trends which resemble the PHY-layer multicasting.

REFERENCES

- [1] E. Karipidis, N. Sidiropoulos and Z.-Q. Luo, "Transmit Beamforming to multiple Co-channel Multicast Groups," *IEEE International Workshop on Computational Advances in Multi-Sensor Adaptive Processing (CAMSAP)*, pp. 109-112, December 2005.
- [2] D. Christopoulos, S. Chatzinotas and B. Ottersten, "Weighted Fair Multicast Multigroup Beamforming under Per-antenna Power Constraints," *IEEE Transactions on Signal Processing*, vol. 62, no. 19, pp. 5132-5142, 2014.
- [3] D. Christopoulos, S. Chatzinotas and B. Ottersten, "Multicast Multigroup Precoding and User Scheduling for Frame-Based Satellite Communications," *IEEE Transactions on Wireless Communications*, vol. 99, no. 99, pp. 1-1, 2015.
- [4] Y. C. B. Silva and A. Klein, "Linear Transmit Beamforming Techniques for the Multigroup Multicast Scenario," *IEEE Transaction on Vehicular Technology*, vol. 58, no. 8, pp. 4353 - 4367, October 2009.
- [5] M. Bengtsson and B. Ottersten, "Optimal and Suboptimal Transmit beamforming," in *Handbook of Antennas in Wireless Communications*, L. C. Godara, Ed. CRC Press, 2001.
- [6] M. Schubert and H. Boche, "Solution of the Multiuser Downlink Beamforming Problem with Individual SINR Constraints," *IEEE Transaction on Vehicular Technology*, vol. 53, pp. 1828, January 2004.
- [7] R. H. Roy and B. Ottersten, "Spatial division multiple access wireless communication systems, *US patent, n°* US 5515378A, 1991.
- [8] D. Gesbert, M. Kountouris, R. W. Heath Jr., C.-B. Chae and T. Sälzer, "From Single User to Multiuser Communications: Shifting the MIMO Paradigm," *IEEE Signal Processing Magazine*, vol. 24 no.5, pp. 36-46, 2007.
- [9] E. Björnson, M. Bengtsson and B. Ottersten, "Optimal Multi-User Transmit Beamforming: Difficult Problem with a Simple Solution Structure," *IEEE Signal Processing Magazine*, vol. 31, no. 4, pp. 142 - 148, 2014.
- [10] A. B. Gershman, N. D. Sidiropoulos, S. Shahbazpanahi, M. Bengtsson, and B. Ottersten, "Convex Optimization Based Beamforming," *IEEE Signal Processing Magazine*, vol. 27, no. 3, pp. 62-75, May 2010.
- [11] Q. H. Spencer, A.L. Swindlehurst, and M. Haardt, "Zero-forcing Methods for Downlink Spatial Multiplexing in Multiuser MIMO Channels," *IEEE Transactions on Signal Processing*, vol. 52, no.2, pp. 461-471, February 2004.
- [12] Q. H. Spencer, C. B. Peel, A.L. Swindlehurst, and M. Haardt, "An Introduction to the Multi-User MIMO Downlink," *IEEE Communications Magazine*, vol. 42, no. 10, pp. 60-67, October 2004.
- [13] A. Wiesel, Y. C. Eldar, and S. Shamai, "Linear precoding via conic optimization for fixed MIMO receivers," *IEEE Transactions on Signal Processing*, vol. 54, no. 1, pp. 161-176, 2006.
- [14] Y. Wu, M. Wang, C. Xiao, Z. Ding and X. Gao, "Linear Precoding for MIMO Broadcast Channels with Finite-Alphabets Constraints," *IEEE Transactions on Wireless Communications*, vol. 11, no. 8, pp. 2906-2920, August 2012.
- [15] H. Boche, and M. Schubert, "Resource allocation in multiantenna systems-achieving max-min fairness by optimizing a sum of inverse SIR," *IEEE Transactions on Signal Processing*, vol. 54 no. 6, pp. 1990-1997, 2006.
- [16] R. Ghaffar and R. Knopp, "Near Optimal Linear Precoding for Multiuser MIMO for Discrete Alphabets," *IEEE International Conference on Communications (ICC)*, pp. 1-5, May 2010.
- [17] C. Masouros and E. Alsusa, "Dynamic Linear Precoding for the exploitation of Known Interference in MIMO Broadcast Systems," *IEEE Transactions On Communications*, vol. 8, no. 3, pp. 1396 - 1404, March 2009.
- [18] C. Masouros, "Correlation Rotation Linear Precoding for MIMO Broadcast Communications," *IEEE Transactions on Signal Processing*, vol. 59, no. 1, pp. 252 - 262, January 2011.
- [19] C. Masouros, M. Sellathurai, and T. Ratnarajah, "Interference optimization for transmit power reduction in Tomlinson-Harashima precoded MIMO downlinks," *IEEE Transactions on Signal Processing*, vol. 60 no. 5, pp. 2470-2481, May 2012.

- [20] M. Alodeh, S. Chatzinotas and B. Ottersten, "Data Aware User Selection in the Cognitive Downlink MISO Precoding Systems," *invited paper to IEEE International Symposium on Signal Processing and Information Technology (ISSPIT)*, December 2013.
- [21] M. Alodeh, S. Chatzinotas and B. Ottersten, "A Multicast Approach for Constructive Interference Precoding in MISO Downlink Channel," *International Symposium in Information theory (ISIT)*, June, 2014.
- [22] M. Alodeh, S. Chatzinotas and B. Ottersten, "Constructive Multiuser Interference in Symbol Level Precoding for the MISO Downlink Channel," *IEEE Transactions on Signal processing*, vol. 63, no. 9, pp. 2239-2253, May, 2015.
- [23] C. Masouros and G. Zheng, "Exploiting Known Interference as Green Signal Power for Downlink Beamforming Optimization," *IEEE Transactions on Signal Processing*, vol. 63, no. 14, pp. 3628-3640, 2015.
- [24] M. Alodeh, S. Chatzinotas and B. Ottersten, "Energy Efficient Symbol-Level Precoding in Multiuser MISO Channels," *accepted in 16th IEEE Int. Workshop on Signal Process. Adv. in Wireless Communications (SPAWC)*, June 2015.
- [25] M. Alodeh, S. Chatzinotas and B. Ottersten, "Energy Efficient Symbol-Level Precoding in Multiuser MISO Channels Based on Relaxed Detection Region," *submitted to IEEE Transactions Wireless Communications*, available on arXiv:1504.06749 [cs.IT], 2015.
- [26] M. Alodeh, S. Chatzinotas and B. Ottersten, "Constructive Interference through Symbol Level Precoding for Multi-level Modulation," *accepted in Globecom 2015*, available on Arxiv arXiv:1504.06750 [cs.IT].
- [27] N. D. Sidiropoulos, T. N. Davidson, and Z.-Q. Luo, "Transmit Beamforming for Physical-Layer Multicasting," *IEEE Transactions on Signal Processing*, vol. 54, no. 6, pp. 2239-2251, June 2006.
- [28] N. Jindal and Z.-Q. Luo, "Capacity Limits of Multiple Antenna Multicast," *IEEE International Symposium on Information Theory (ISIT)*, pp. 1841 - 1845, June 2006.
- [29] B. Du, M. Chen, W. Zhang and C. Pan, "Optimal beamforming for single group multicast systems based on weighted sum rate," *IEEE International Conference on Communications(ICC)*, pp. 4921- 4925, June 2013.
- [30] E. Jorswieck, "Beamforming in Interference Networks: Multicast, MISO IFC and Secrecy Capacity," *International Zurich Seminars (IZS)*, March 2011.
- [31] A. R. Forouzan, M. Moonen, J. Maes and M. Guenach, "Joint Level 2 and 3 Dynamic Spectrum Management for Downstream DSL," *IEEE Transactions on Communications*, vol. 60, no. 10, pp.3111-3122, October 2012.
- [32] A. Garcia- Armada, "SNR Gap Approximation for M-PSK-Based Bit Loading," *IEEE Transactions on Wireless Communications*, vol. 5, no.1, pp. 57-60, January, 2006.
- [33] S. Boyd, and L. Vandenberghe, *Convex Optimization*, Cambridge University press.
- [34] J. Proakis, *Digital Communications*, 4th Edition.
- [35] O. Afelumo, A. B. Awoseyila, and B. G. Evans, "Simplified evaluation of APSK error performance," *IET electronic letters*, vol. 48, no. 14, pp. 886 - 888, July 2012.
- [36] A. Checko, H.L. Christiansen, Yan Ying, L. Scolari, G. Kardaras, M.S. Berger, and L. Dittmann, "Cloud RAN for Mobile NetworksA Technology Overview," *IEEE Communications Surveys & Tutorials*, Vol. 17, no. 1, pp. 405 - 426, First quarter, 2015.